Decay rates of excited muonic molecular ions

E. Lindroth,[1] J. Wallenius,[2] and S. Jonsell[3]
[1]*Department of Atomic Physics, Stockholm University, Stockholm, Sweden*
[2]*Department of Nuclear and Reactor Physics, Royal Institute of Technology, Stockholm, Sweden*
[3]*Department of Physics, University of Umeå, Umeå, Sweden*
(Received 8 May 2003; published 8 September 2003)

Muonic molecular ions in excited states have been predicted to form in collisions between excited muonic atoms and hydrogen molecules. We have calculated radiative and Coulombic decay rates for $pp\mu^*$ and $dd\mu^*$ molecular states located below the $2s$ threshold, using the complex rotation method. The x-ray spectrum from the radiative decay is shown to exhibit several maxima, corresponding to the vibrational motion of the decaying molecule. The branching ratio of the radiative decay mode was calculated to be less than 15% for $pp\mu^*$, while a radiative yield of more than 80% is predicted for the decay of $dd\mu^*$. Our results have a significant impact on the analysis of the muon catalyzed fusion cycle as well as on the interpretation of exotic hydrogen spectroscopy.

DOI: 10.1103/PhysRevA.68.032502 PACS number(s): 36.10.Dr, 33.80.Eh, 33.50.−j

I. INTRODUCTION

When muons enter a mixture of hydrogen, muonic hydrogen atoms are formed in highly excited states. The atoms are deexcited in a so-called cascade by several competing processes including radiative decay [1–3]. After the muon has reached the ground state, muonic molecular formation may take place in collisions of the muonic atom with ordinary hydrogen molecules.

In a recent PSI experiment the kinetic-energy distribution of $p\mu(1s)$ atoms in hydrogen gas was measured for the first time, and a distinct high-energy component in the vicinity of 900 eV was detected [4]. Considering that the direct Coulomb deexcitation,

$$p\mu(2l)+p\rightarrow p\mu(1s)+2 \text{ keV}, \tag{1}$$

has a cross section more than four orders of magnitude too small to explain the observed yield of high-energy $p\mu(1s)$ atoms [5,4], the only feasible source of acceleration to this kinetic energy is the Coulombic decay of muonically excited molecular states:

$$pp\mu^*\rightarrow p\mu(1s)+p+2 \text{ keV}, \tag{2}$$

and such $pp\mu^*$ states thus must form with a significant probability during the cascade. In fact, it has been predicted that resonant formation of $dt\mu^*$ molecules in collisions of $t\mu(2s)$ with ordinary D_2 would constitute an important ''side path'' in the muon catalyzed fusion cycle, explaining the discrepancy between measured and calculated muon cycling rates [6–8].

In order to further explore the presence of the side path in muonic hydrogen cascades, Pohl and co-workers conducted a test experiment in D_2 [9]. No clear signal of a high-energy component was detected, which at first seemed puzzling. However, it has been predicted that the Coulombic decay rate (2) for excited $dd\mu$ molecules is more than two orders of magnitude smaller than for $pp\mu^*$ [10]. Thus it can be expected that in D_2, the radiative decay branch,

$$dd\mu^*\rightarrow d\mu(1s)+d+\gamma+2 \text{ keV}, \tag{3}$$

should dominate. The exact branching ratio has remained unknown until now.

In the present paper we calculate radiative and Coulombic decay rates of $pp\mu^*$and $dd\mu^*$ molecular states located below the $2s$ threshold. First we give an account of the methods used. Then we display the calculated rates, branching ratios, and x-ray spectra. Finally we discuss the impact of our results on the analysis of the muon catalyzed fusion cycle and precision experiments in exotic hydrogen.

II. METHOD

The solution to the nonrelativistic Schrödinger equation for the three-body problem was found using two different methods: by the coupled rearrangement channel method with Gaussian basis functions (CRC-GB) [11] and by diagonalization of the three-particle Hamiltonian with a spherical basis set centered around the muon and the radial part expanded in B splines [12]. In both cases complex rotation is used to treat the inherently in-stable molecular states and the Coulombic widths are obtained from the imaginary part of complex energy eigenvalues.

A. The coupled rearrangement channel method

In the symmetrized CRC-CB method [13], the three-body wave function $\Psi^{pq}_{JM_J}$ of total orbital angular momentum J is expanded in Gaussian basis functions spanned over the possible rearrangement channels α shown in Fig. 1:

$$\Psi^{pq}_{JM_J}=\sum_{\alpha ilIL}\frac{c_{\alpha ilIL}}{\sqrt{2}}[1+q(-1)^J\mathcal{I}_n]g_{\alpha ilIL}, \tag{4}$$

$$g_{\alpha ilIL}=r_\alpha^l R_\alpha^L e^{-(r_\alpha/r_{\alpha_i})^2-(R_\alpha/R_{\alpha_I})^2}[Y_l(\hat{\mathbf{r}}_\alpha)\otimes Y_L(\hat{\mathbf{R}}_\alpha)],$$

where r_{α_i} and R_{α_I} are nonlinear variational parameters and $\mathcal{I}_n$ is the nuclear coordinate inversion operator. The quantum numbers p and q are defined through

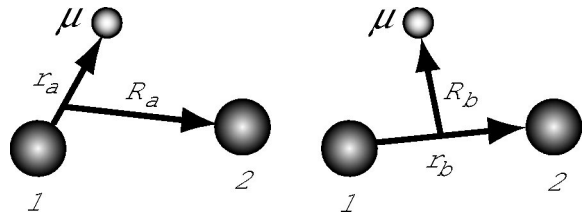

FIG. 1. Jacobian coordinates of the muonic three-body system, written in the two rearrangement channels *a* and *b*.

$$\mathcal{I}\Psi^{pq}_{JM_J} = p(-1)^J \Psi^{pq}_{JM_J}, \tag{5}$$

$$\mathcal{I}_n \Psi^{pq}_{JM_J} = q(-1)^J \Psi^{pq}_{JM_J}, \tag{6}$$

where operation with $\mathcal{I}$ implies inversion of *all* spatial coordinates.

The three-body state can be classified as *gerade/ungerade* according to whether $pq = \pm 1$. This approach requires comparatively few terms in the partial-wave expansion, and enables a good description of molecular levels near the dissociation threshold. The version of the CRC-GB code that we have used does not, however, enable calculation of photodecay widths, for which we have instead used the *B*-spline method.

B. The *B* spline method

In the *B* spline method, $pp\mu$ and $dd\mu$ molecules are treated as is customary to treat the H^- ion (eep), but with light and heavy particles interchanged. Although this approach leads to rather slow convergence in terms of partial waves, it has the advantage that the calculation is made in a framework where photodecay can easily be accounted for. We outline here the special considerations necessary to treat the $pp\mu$ molecule, referring to Ref. [12] for details.

In the center of mass frame the full three-particle Hamiltonian reads

$$H = \frac{\mathbf{p}_1^2}{2\mu} + \frac{\mathbf{p}_2^2}{2\mu} + \frac{\mathbf{p}_1 \cdot \mathbf{p}_2}{m_\mu} + \frac{e^2}{4\pi\varepsilon_0}\left(\frac{1}{r_{12}} - \frac{1}{r_{1\mu}} - \frac{1}{r_{2\mu}}\right), \tag{7}$$

where $\mu = m_p m_\mu/(m_p + m_\mu)$. The problem is solved in two steps. First, eigenfunctions to the $p\mu$ two-body problem are constructed. A *B*-spline basis set is used to expand the radial functions. They are piecewise polynomials defined on a so-called knot sequence, chosen for the system to be studied, and form a complete set on this knot sequence. During the last decade *B*-splines have been used extensively in atomic and molecular physics, see Ref. [14] for a review. The expansion is obtained by diagonalization, after conversion of the differential equation to a generalized symmetric eigenvalue equation. In the second step these eigenfunctions are coupled to total orbital angular momentum and spin and used as a basis set to expand the eigenfunctions of Hamiltonian (7) in terms of partial waves. The eigenfunctions are finally found by diagonalization of a symmetric matrix. This procedure follows closely the method presented for negative ions in Ref. [12], the main difference being the importance of the mass-polarization term $\mathbf{p}_1 \cdot \mathbf{p}_2$. For a muonic molecule this term cannot be neglected, and the operator couples strongly terms in the partial-wave expansion that differ with one unit in the individual angular momenta. The result is a slower convergence of the partial-wave expansion compared to atoms where the mass polarization term is small. Partial waves with $\ell = 7-8$, are here required to obtain convergence.

To calculate the width for photodissociation we use a procedure originating from Rescigno and McKoy [15]. They have shown how the photoabsorption cross section, in the framework of complex scaling, can be obtained as the imaginary part of the dynamic polarizability. Due to symmetry under time inversion the expression can easily be reformulated to apply to photon emission. Since the interest here is the decay to the continuum, the quantity to consider is the decay rate per unit photon energy dA/dE_γ. Applying the dipole approximation for describing the interaction with the photon field one has

$$\frac{dA(\hbar\omega)}{d(\hbar\omega)} = \frac{e^2}{4\pi\epsilon_0}\frac{4}{3\pi\hbar^4}\frac{(\hbar\omega)}{c^3}(E_n - E_r)^2 \times \mathrm{Im}\left(\sum_n \frac{\langle \Psi_n | \sum_j \mathbf{r}_j e^{i\theta} | \Psi_r \rangle^2}{E_n + \hbar\omega - E_r}\right), \tag{8}$$

where θ is a complex rotation angle large enough to uncover the resonances for which decay rates are calculated and the functions Ψ are eigenstates to the rotated Hamiltonian (7) with complex eigenvalues E. E_r denotes the complex energy eigenvalue of the resonance, having a width $\Gamma_r = 2\,\mathrm{Im}[E_r]$. A discretized description of the continuum is used and it is thus enough to sum over final states *n*.

III. RESULTS

The three-body resonances considered here are situated below the $2s$ state of muonic hydrogen or deuterium. They are expected to form via the Vesman mechanism [16,17] in collisions of a muonic atom in the $2s$ state with ordinary hydrogen molecules according to, e.g.,

$$p\mu(2s) + H_2 \rightarrow [(pp\mu^*)^{pq}_{vJ} - pee]_{\nu K}, \tag{9}$$

where *J* is the total orbital angular momentum of the muonic molecule acting as a pseudonucleus of the rovibrationally excited host molecule. If the nuclei are identical, the Born-Oppenheimer approximation may be applied to classify vibrational states v of the resonances. States of gerade symmetry $(pq = 1)$ are then supported by the $3d\sigma_g$ potential and those of ungerade symmetry $(pq = -1)$ by the $4f\sigma_u$ potential [18,19,13]. In Fig. 2, the corresponding potential curves are plotted in atomic units.

The metastable resonances are stabilized towards back decay by emission of an Auger electron from the host molecule:

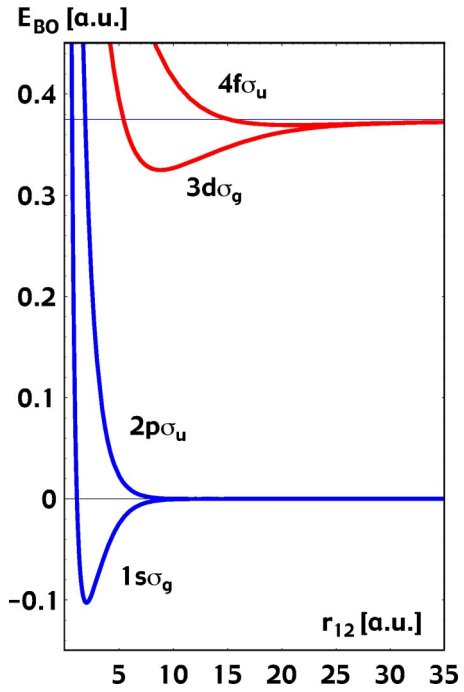

FIG. 2. (Color online) Born-Oppenheimer potential energy as a function of internuclear distance. The muonic atomic unit for length is $a_0\mu_e/\mu_\mu$, with μ_e and μ_μ being the reduced mass of hydrogen and muonic hydrogen, respectively. Energies are given in atomic units relative to the $1s$ threshold. In the muonic system, one atomic energy unit equals (μ_μ/μ_e) hartree.

$$[(pp\mu^*)_{vJ}^{pq} - pee]_{\nu K} \rightarrow [(pp\mu^*)_{v'J'}^{pq'} - pe]_{\nu' K'}^{+} + e^-. \tag{10}$$

After emission of a second Auger electron, the only possible decay modes are dissociation with and without photoemission, which hence takes place from states located more than 15.4 eV (the ionization energy of the hybrid molecule) below the $2s$ threshold. Thus, we limit our present investigation to the decay widths of gerade states having total orbital angular momentum $J=0$ or 1, i.e, to states supported by the $3d\sigma_g$ potential in Fig. 2.

In atomic physics, the usual label for a $J=0$ gerade state is $^1S^e$. S corresponds to zero total orbital angular momentum and 1 denotes that the spins of the two protons are coupled to zero. The gerade/ungerade symmetry is the combined effect of spin and parity, $\pi(-1)^S$, where plus and minus gives gerade and ungerade, respectively. The atomic label for a $J=1$ gerade state is $^3P^o$. Although deuterons are spin-1 bosons the translation works for $dd\mu$ too since the different symmetry of the total bosonic wave function with respect to exchange of the two identical particles is compensated by the opposite symmetry of the spin wave function. The symmetry of the spatial wave function is thus unchanged when $pp\mu$ is replaced with $dd\mu$; $J=0$ gerade and $^1S^e$ still denote the same state.

The muon is strongly localized to one of the heavy particles. Its state resembles a mixture of the atomic $2s$ and $2p$ states, and is only weakly perturbed by the second heavy particle. Radiative decay occurs to states with opposite parity and with the spin-alignment unchanged, i.e., to states supported by opposite gerade-ungerade symmetry potential. States supported by the $3d\sigma_g$ potential can thus only decay to the $2p\sigma_u$ potential. This potential is antibonding and supports no bound states. The only possibility is thus decay to the continuum. Qualitatively this can be described as a muonic transition to an atomic ground state leaving the other heavy particle in a repulsive potential. This decay mode is more or less independent of the mass ratio between the light and heavy particles. To autodissociate without emission of a photon, i.e., Coulombic decay, the two heavy particles have to exchange momentum, an event that has significant probability only when they come close to each other. This process is thus strongly dependent on the wave function for the particular resonance state as well as of the mass ratio [10]. The corresponding process in H^-, autodetachment, dominates by many orders of magnitude over photodetachment. We show here that for $pp\mu^*$ autodissociation is still more important than photodissociation, while the decay of $dd\mu^*$ is dominated by photodissociation. Table I displays the calculated energies and decay rates of $pp\mu^*$ states with zero total orbital angular momentum. The energy and the Coulombic decay rates are obtained by CRC-GB. Hilico has recently calculated the energies of these states with an orthogonal basis set, allowing for an accuracy in the μeV range [20]. The energies calculated by Hilico are quoted in Table I and as can be seen, our results differ from Hilico's by no more than 1 meV in the real part of the energy.

The widths for photodissociation were calculated with the B-spline method. They are larger than the radiative width for atomic $p\mu(2p)$, $\Gamma_\gamma^{2p\rightarrow 1s}=0.12$ ps^{-1}. We interpret this as

TABLE I. Energies, decay rates, and radiative decay yields $\Upsilon_\gamma=\Gamma_\gamma/(\Gamma_{\mathrm{Coul}}+\Gamma_\gamma)$ for gerade states of $pp\mu^*$ with $J=0$. The energies are given in eV relative to the $p\mu(2s)$ threshold and decay rates are given in units of per picosecond. The two columns to the right quote energies and decay rates calculated by Hilico.

$E_r(^1S^e)$	Γ_{Coul}	Γ_γ	Υ_γ	$E_r(^1S^e)$	Γ_{Coul}
−191.616	2.59	0.257	0.09	−191.615	2.59
−93.046	4.49	0.220	0.05	−93.045	4.49
−31.960	3.40	0.205	0.06	−31.960	3.52
−9.009	1.02	0.207	0.16	−9.009	1.05
−2.789	0.31			−2.789	0.33
−0.878	0.15			−0.878	0.10

TABLE II. Energies, decay rates, and radiative decay yields $\Upsilon_\gamma=\Gamma_\gamma/(\Gamma_{\mathrm{Coul}}+\Gamma_\gamma)$ for gerade states of $pp\mu^*$ with $J=1$. The energies are given in eV relative to the $p\mu(2s)$ threshold and decay rates are given in units of per picoseconds. The two columns to the right quote energies and decay rates calculated by Hilico.

$E_r(^3P^o)$	Γ_{coul}	Γ_γ	Υ_γ	$E_r(^3P^o)$	Γ_{Coul}
−181.468	2.14	0.252	0.11	−181.468	1.85
−85.839	3.53	0.216	0.06	−85.839	2.97
−27.831	2.46	0.205	0.08	−27.831	2.12
−7.558	0.62	0.208	0.25	−7.558	0.58
−2.254				−2.253	
−0.684				−0.290	

sizable contributions to the transition matrix element from other configurations than the asymptotic muon orbitals in the initial and final states. As explained above, the radiative widths are less sensitive to the exact shape of the wave function and have an estimated uncertainty of less than 1%. The branching ratio into the radiative decay channel is hence predicted to be in the range of 5–10% for the Auger stabilized states of $pp\mu^*$, i.e., when $E_r\lesssim -15.4$ eV.

Table II shows the calculated energies and decay rates of $pp\mu^*$ states with total orbital angular momentum $J=1$. We were not able to obtain reliable widths with the CRC-GB method in this case, and hence the Coulombic decay rates for these $^3P^o$ states were calculated with the *B*-spline method. The rates differ by up to 20% from the results of Hilico [20]. The widths for photodissociation were calculated with the *B*-spline method as in the case of $J=0$ and do not depend significantly on the total orbital angular momentum. In spite of the uncertainty in the Coulombic decay rates calculated by us, we may predict that the radiative yield in the decay of Auger stabilized $^3P^o$ states remains below 15%.

In Table III the corresponding results for ^1S states of $dd\mu^*$ are shown. The binding energies were obtained with the CRC-GB method, and are equal to or lower than those calculated by Hara and Ishihara [19]. The radiative widths were obtained with the *B*-spline method and deviate by less than 20% from the corresponding $pp\mu^*$ widths.

The Coulombic decay rates for $dd\mu^*$ calculated with CRC-GB, are very small, and even with the largest basis set that could be applied (5800 basis functions), variations in the width of up to a factor of 2 was registered for different real scaling parameters, using the condition $dE/d\theta=0$ to identify the resonance location. In order to discriminate between the suggested widths, the complex eigenvalue with the lowest real part was selected and quoted in Table III. Considering that Gailitis' prediction of a constant ratio between the widths as function of vibrational quantum number appears to be valid for the higher vibrational states [21,20], we estimate that the error in the quoted $dd\mu^*$ widths is less than 50%. Our results thus support the prediction that Coulombic widths of $^1S^e$ $dd\mu^*$ states are more than two orders of magnitude smaller than for $^1S^e$ $pp\mu^*$ states [10].

In the Born-Oppenheimer (BO) approximation, the resonant states supported by $3d\sigma_g$ potential are orthogonal to the continuum states of the $2p\sigma_u$ as well as the $1s\sigma_g$ potential, being different eigenstates to the same Hamiltonian. The $3d\sigma_g$ states would therefore have an infinite Coulombic lifetime in the BO-picture. With a full three-body Hamiltonian, gerade and ungerade states are still orthogonal, while transitions between approximate $3d\sigma_g$ and $1s\sigma_g$ states are allowed. The larger mass difference between the muon and the nuclei makes the BO approximation more accurate for $dd\mu^*$ than in the case of $pp\mu^*$, hence the smaller Coulombic decay rate.

Fortunately, the radiative yield is not very sensitive to the Coulombic width within the estimated uncertainty, and we predict branching ratios into the radiative channel of more than 80% for $dd\mu^*$.

The wave functions of the metastable molecular states may be illustrated in terms of the probability density function for the internuclear distance r_{12}

$$P(r_{12})=r_{12}^2\int |\Psi(r_\mu,r_{12})|^2 d\mathbf{r}_\mu d\hat{\mathbf{r}}_{12}, \tag{11}$$

being normalized as

TABLE III. Complex energies, decay rates, and radiative decay yields $\Upsilon_\gamma=\Gamma_\gamma/(\Gamma_{\mathrm{Coul}}+\Gamma_\gamma)$ for $^1S^e$ gerade states of $dd\mu^*$. The energies are given relative to the $d\mu(2s)$ threshold.

E_r (eV)	E_i (μeV)	Γ_{Coul} (ps^{-1})	Γ_γ (ps^{-1})	Υ_γ
−218.112	−0.9	0.003	0.271	0.99
−135.279	−6.6	0.020	0.229	0.92
−72.967	−12.9	0.040	0.210	0.84
−31.902	−14.0	0.043	0.209	0.83
−12.617	−5.8	0.018	0.217	0.92
−5.311	−2.6	0.008		

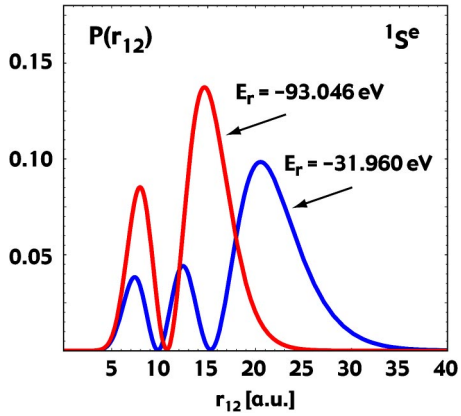

FIG. 3. (Color online) Probability density $P(r_{12})$ for the internuclear distance of Auger stabilized $pp\mu^*$ $^1S^e$ states with gerade symmetry.

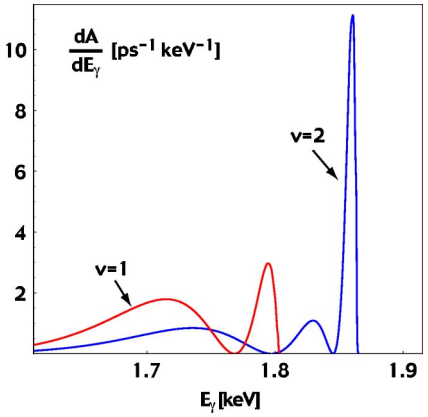

FIG. 4. (Color online) Predicted x-ray spectra from the decay of gerade $^1S^e$ $pp\mu^*$ states. The area under each curve equals the total photodecay rate from that state.

$$\int P(r_{12})dr_{12}=1. \tag{12}$$

In Fig. 3, $P(r_{12})$ is plotted for the first and second vibrationally excited $^1S^e$ $pp\mu^*$ states. Comparing Figs. 3 and 2 one may note that the energy of the final state after a radiative decay will contain a kinetic-energy component determined by the distance between the nuclei at the instant of decay. In the Born-Oppenheimer approximation, the photon energy E_γ is given by

$$E_\gamma=E_{pp\mu^*}-E_{2p\sigma_u}(r_{12}), \tag{13}$$

where r_{12} is the internuclear distance and $E_{2p\sigma_u}$ is the repulsive potential of the final state. For large distances, E_γ approaches

$$E_\gamma^{\max}=E_{pp\mu^*}-E_{p\mu(1s)}. \tag{14}$$

For small distances the energy is given by the inner turning point R_i of the initial state:

$$E_\gamma^{\min}\simeq E_{pp\mu^*}-E_{2p\sigma_u}(R_i). \tag{15}$$

The x-ray spectrum thus is spread out over several hundred electron volts, with minima corresponding to nodes in the vibrational motion of the initial state.

The calculated spectra of x rays from the decay of the Auger stabilized $pp\mu^*$ states depicted in Fig. 3 are shown in Fig. 4. The area under each curve equals the total photodecay rate from that state. Comparing Figs. 3 and 4, one may note that the probability for photodecay is increased for smaller internuclear distances. For, e.g., $v=1$, the probability to find the nuclei at a distance smaller than 10 a.u. is about one third, while radiative decay occurring in this range provides more than 80% of the total rate. For such distances, the muon orbitals in initial and final states contain components different from the asymptotic configurations, explaining the large value of the transition matrix element.

We are not aware of any other calculations of photodissociation rates for muonic hydrogen molecules. The predicted rates for muonic hydrogen molecules are similar to the muonic helium hydride rates calculated by Hara and Ishihara [22], which may be explained by the fact that the larger photon energy in the latter case compensates for the smaller transition matrix element. The spread of the helium hydride x-ray spectrum is larger, since the inner turning point of the initial state is much smaller.

IV. CONCLUSIONS

In conclusion, we have calculated widths for radiative decay of $pp\mu^*$ and $dd\mu^*$ metastable states situated below the $2s$ threshold. The decay rate is a function of initial vibrational state, varying between 0.2 and 0.3 ps^{-1}. The dependence on angular momentum and reduced mass is rather weak. Our calculated values of Coulombic decay rates support earlier work showing that these rates for $dd\mu^*$ are orders of magnitude smaller than for $pp\mu^*$ [10]. We predict a branching ratio into the photodissociation channel smaller than 15% for $pp\mu^*$ and larger than 80% for $dd\mu^*$. Such branching ratios appear to explain PSI experiments detecting, on one hand, high-energy ground-state atoms in the the muonic hydrogen cascade and, on the other hand, the absence of such atoms in the muonic deuterium cascade [4,9].

The possibility of the direct (nonmolecular) Coulomb deexcitation process,

$$p\mu(n=2)+p\rightarrow p\mu(1s)+p+2\ \text{keV}, \tag{16}$$

to be responsible for the population of $p\mu(1s)$ atoms with high kinetic energy detected in the experiment is highly unlikely, since the magnitude of the cross section is vanishingly small at the $n=2$ level. The PSI measurement indicates that a Coulombic deexcitation rate for $p\mu(2s)$ atoms at liquid hydrogen density (LHD) of the order of 4×10^{11} s^{-1} would be required to explain the results of the experiment [4]. The value of the direct Coulomb deexcitation rate obtained by extrapolation from higher n is however of the order of 10^7-10^8 s^{-1} [23,5]. It should here be noted that the rates published by Bracci and Fiorentini in Ref. [24] ($\sim10^{10}$ s^{-1} at $n=2$) are completely unreliable, due to the use of approxi-

mations outside the range of their validity. The rate $\sim 10^{10}\ s^{-1}$ at $n=3$ published by Ponomarev and Solovev [25] has later been corrected downwards by two orders of magnitude in a joint work with Kravtsov and Mikhailov [5].

Hence, we believe that our results provide strong evidence for muonic molecular formation taking place in collisions of excited muonic atoms with hydrogen. When modeling the kinetics of the muon catalyzed fusion cycle, one must thus take into account a significant fraction of radiation free decay from $n=2$ to $n=1$, yielding 900-eV muonic atoms in the ground state, as well as a distribution of recoil energies in the few hundred eV range from molecular photodecay. In the $dt\mu$ cycle, the latter effect is expected to be the most prominent, considering that Coulombic decay rates of the $dt\mu^*$ molecule are similar to those of $dd\mu^*$ [26]. Experiments having measured the probability for the muon to reach the $p\mu(1s)$ level in HD mixtures, i.e., the q_{1s} quantity, should be reanalyzed to take into account the radiation free branch of the $p\mu(2s)$ deexcitation [27,28]. The formation of metastable molecular states during exotic hydrogen cascade will also require a modified analysis of exotic hydrogen spectroscopy, with impact on high-precision experiments aiming at measuring weak and strong force properties. We finally note that high-resolution ($\Delta E \lesssim 10$ eV) measurements of x-ray spectra in D_2 at suitable densities may give direct information on feed rates to the dissociating $dd\mu^*$ states. Such measurements may be feasible using crystal spectrometers [29].

ACKNOWLEDGMENTS

The authors wish to thank R. Pohl, F. Kottmann, V. Markushin, L. Hilico, and P. Froelich for illuminating discussions. The original CRC-GB code was kindly supplied by M. Kamimura. This work was supported by the Swedish Science Council (VR).

[1] M. Leon and H. Bethe, Phys. Rev. **127**, 636 (1962).
[2] V. Markushin, Phys. Rev. A **50**, 1137 (1994).
[3] V. Markushin and T. Jensen, Hyperfine Interact. **138**, 71 (2001).
[4] R. Pohl *et al.*, Hyperfine Interact. **138**, 35 (2001).
[5] A. Kravtsov, A.I. Mikhailov, L.I. Ponomarev, and E.A. Solovev, Hyperfine Interact. **138**, 99 (2001).
[6] P. Froelich, Adv. Phys. **41**, 1 (1992).
[7] P. Froelich and J. Wallenius, Phys. Rev. Lett. **75**, 2108 (1995).
[8] J. Wallenius and P. Froelich, Phys. Rev. A **54**, 1171 (1996).
[9] R. Pohl, in *Proceedings of the Workshop on Molecular Effects in the Exotic Hydrogen Cascade*, edited by R. Pohl (PSI, Villigen, 2001).
[10] O. Tolstikhin, I. Tolstikhina, and C. Namba, Phys. Rev. A **60**, 4673 (1999).
[11] M. Kamimura, Phys. Rev. A **38**, 621 (1988).
[12] J. Sanz-Vicario, E. Lindroth, and N. Brandefelt, Phys. Rev. A **66**, 052713 (2002).
[13] S. Jonsell, J. Wallenius, and P. Froelich, Phys. Rev. A **59**, 3440 (1999).
[14] H. Bachau *et al.*, Rep. Prog. Phys. **64**, 1601 (2001).
[15] T. Rescigno and V. McKoy, Phys. Rev. A **12**, 522 (1975).
[16] E. Vesman, JETP Lett. **5**, 91 (1967).
[17] J. Wallenius, S. Jonsell, Y. Kino, and P. Froelich, Hyperfine Interact. **138**, 285 (2001).
[18] I. Shimamura, Phys. Rev. A **40**, 4863 (1989).
[19] S. Hara and T. Ishihara, Phys. Rev. A **40**, 4232 (1989).
[20] L. Hilico, N. Billy, B. Gremaud, and D. Delande, in *Proceedings of the Workshop on Molecular Effects in the Exotic Hydrogen Cascade* (Ref. [9]).
[21] M. Gailitis and R. Damburg, Proc. Phys. Soc. London **82**, 192 (1963).
[22] S. Hara and T. Ishihara, Phys. Rev. A **39**, 5633 (1989).
[23] W. Czaplinski *et al.*, Phys. Rev. A **50**, 525 (1994).
[24] L. Bracci and G. Fiorentini, Nuovo Cimento **43**, 9 (1978).
[25] L. Ponomarev and E. Solovev, JETP Lett. **68**, 7 (1998).
[26] Y. Kino and M. Kamimura, Hyperfine Interact. **102**, 191 (1996).
[27] B. Lauss *et al.*, Phys. Rev. Lett. **80**, 3041 (1998).
[28] S. Sakamoto, K. Ishida, and K. Nagamine, Phys. Lett. A **260**, 253 (1999).
[29] L. Simons, Hyperfine Interact. **119**, 281 (1999).